Large Eddy Simulation of Fluid flow and Heat Transfer in the Upper Plenum of Fast Reactor

Dong-Eun Kim [a*], Sung-Ho Ko [b], Seok-Ki Choi [a], Tae-Ho Lee [a]
[a]*Korea Atomic Energy Research Institute, Yuseong, Daejeon, Republic of Korea*
[b]*Chungnam National University, Yuseong, Daejeon, Republic of Korea*

[*]*Corresponding author: kdepirate@hanmail.net*

1. Introduction

There are many complicated components in the upper plenum of the PGSFR (Prototype Generation-IV Sodium-cooled Fast Reactor) being developed at KAERI (Korea Atomic Energy Research Institute). The temperature differences of the fluid which flows out the fuel assemblies, control rod assemblies and blanket subassemblies form the fluctuations of temperature and leads to thermal fatigue at the solid wall of the structures in the upper plenum. Likewise, the temperature fluctuation transferred to the solid wall can cause a high cycle thermal fatigue. This phenomenon is called thermal striping. The important parameters in the thermal striping are the frequency and the amplitude of the temperature fluctuation. Since the sodium used as coolant in the PGSFR has a high thermal conductivity, the temperature fluctuation can be easily transferred to the solid walls of the components in the upper plenum. To remedy these problems, numerical studies are performed in the present study to analyze the thermal striping for possible improvement of the design and safety of the reactor.

Several experimental and numerical works have been done in the past to understand the phenomenon of thermal striping. As experimental work, Nam and Kim [1] in KAERI provided detailed experimental data for the thermal striping, mainly to test the turbulence models and LES method. The types of test sections are a planar double-jet and a planar triple-jet, and the working fluid is air. For the numerical works, Chacko et al. [2] performed LES for the experiment by Nam and Kim [1], and found that the LES can produce the oscillation of temperature fluctuation properly, while the realizable $k-\varepsilon$ model [3] predicts the amplitude and frequency of the temperature fluctuation very poorly indicating that the LES method is an appropriate calculation method for the thermal striping.

In this paper, the simulation of thermal striping in the upper plenum of PGSFR is performed using the LES method. The WALE eddy viscosity model by Nicoud and Ducros [4] built in CFX-13 commercial code is employed for the LES eddy viscosity model.

2. Governing Equations

In the LES method, the governing equations for the conservation of mass, momentum and energy for an incompressible flow can be written as follows:

$$\frac{\partial}{\partial x_j}(\rho \overline{U_j}) = 0 \tag{8}$$

$$\frac{\partial}{\partial t}(\rho \overline{U_i}) + \frac{\partial}{\partial x_j}(\rho \overline{U_i}\overline{U_j}) = -\frac{\partial \overline{P}}{\partial x_i} + \frac{\partial}{\partial x_j}\left(\mu \frac{\partial \overline{U_i}}{\partial x_j}\right) - \rho \frac{\partial \overline{\tau_{ij}}}{\partial x_j} \tag{9}$$

$$\frac{\partial}{\partial t}(\rho \overline{\Theta}) + \frac{\partial}{\partial x_j}(\rho \overline{U_j}\overline{\Theta}) = \frac{\partial}{\partial x_j}\left(\frac{\kappa}{Cp}\frac{\partial \overline{\Theta}}{\partial x_j}\right) - \rho \frac{\partial \overline{h_j}}{\partial x_j} \tag{10}$$

where $\overline{f}$ is the filtered quantity defined as follows:

$$\overline{f}(x_i,t) = \iiint_{vol} G(x_i - x_i')\, f(x_i',t)\, dx_i' \tag{11}$$

In the WALE eddy viscosity model by Nicoud and Ducros [16], $\overline{\tau_{ij}}$ in Eq.(9) and $\overline{h_j}$ in Eq.(10) are written as follows:

$$\overline{\tau_{ij}} - \frac{\delta_{ij}}{3}\overline{\tau_{kk}} = -2\,\overline{\nu_t}\,\overline{S_{ij}} = -\overline{\nu_t}\left(\frac{\partial \overline{U_i}}{\partial x_j} + \frac{\partial \overline{U_j}}{\partial x_i}\right) \tag{12}$$

$$\overline{h_j} = -\frac{\overline{\nu_t}}{\mathrm{Pr_t}}\left(\frac{\partial \overline{\Theta}}{\partial x_j}\right) \tag{13}$$

and the eddy viscosity is obtained as follows:

$$\overline{\nu_t} = (C_w \Delta)^2 \frac{\left(S_{ij}^d\, S_{ij}^d\right)^{3/2}}{\left(\overline{S_{ij}}\,\overline{S_{ij}}\right)^{5/2} + \left(S_{ij}^d\, S_{ij}^d\right)^{5/4}} \tag{14}$$

where

$$S_{ij}^d = \overline{S_{ik}}\,\overline{S_{ki}} + \overline{\Omega_{ik}}\,\overline{\Omega_{ki}} - \frac{1}{3}\delta_{ij}\left(\overline{S_{mn}}\,\overline{S_{mn}} - \overline{\Omega_{mn}}\,\overline{\Omega_{mn}}\right) \tag{15}$$

$$\overline{S_{ij}} = \frac{1}{2}\left(\frac{\partial \overline{U_i}}{\partial x_j} + \frac{\partial \overline{U_j}}{\partial x_i}\right), \quad \overline{\Omega_{ij}} = \frac{1}{2}\left(\frac{\partial \overline{U_i}}{\partial x_j} - \frac{\partial \overline{U_j}}{\partial x_i}\right) \tag{16}$$

and

$$\Delta = (Vol)^{1/3}, \qquad C_w = 0.55 \sim 0.60 \tag{17}$$

3. Methods and Results

3.1 Numerical method

The geometry and the numerical grid for analysis are generated using the CATIA and CFX-Mesh commercial code respectively. The number of unstructured numerical grid amounts to approximately 2.4 million. The numerical analysis is performed with the CFX-13 commercial code. For the LES method, the convection terms are treated by a central difference scheme and the unsteady terms are treated by the second-order backward Euler difference scheme. The WALE eddy viscosity model is used for the simulation. The size of the time step is 0.0005 seconds and we believe that it is a pretty much small enough to capture the temperature fluctuation.

3.2 Geometries and numerical grid

In this section, some of the geometries used to analyze the problem are illustrated with a short description. The fluid domain for this analysis is a hot pool and that is the section A in Fig. 1, which is the hot pool of the PGSFR.

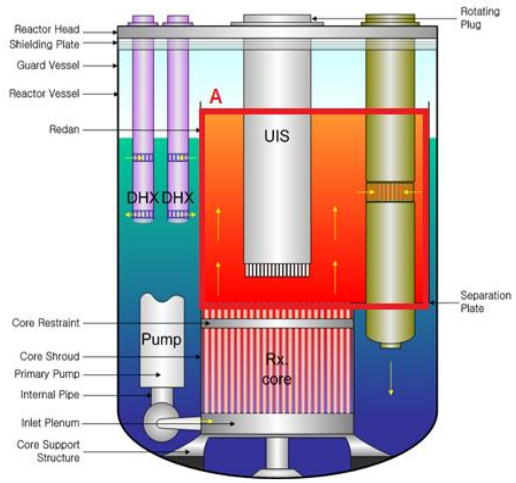

Fig. 1 Schematic diagram of the PHTS

The geometry of the fluid domain is given in Fig. 2 and it consists of a UIS (Upper Internal Structure) in which the control rod shroud tubes are placed vertically and four IHX (Intermediate Heat Exchanger) as a major structure. The inlet of the fluid domain is the core outlet on the bottom of the fluid domain. The core outlet has different conditions in temperature and mass flow rate and the number of assemblies is 253. The inlets of each IHX are the outlet of the solution domain. The inner flow and heat transfer in each IHX are not considered. The UIS has a lot of flow holes on the side wall and the grid plates also have numerous flow holes. The overall views of the UIS and the grid plates are given in Fig. 3. Fig. 4 shows the numerical grid used in the present calculation and the numerical grids are generated by the CFX-Mesh commercial code.

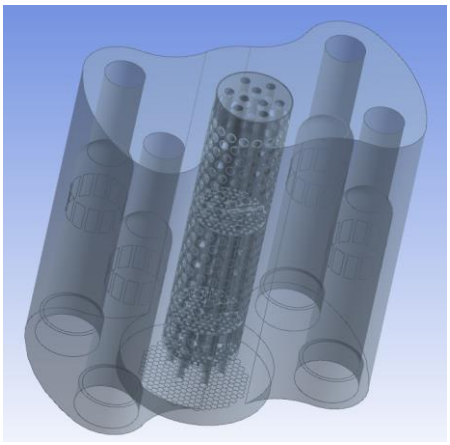

Fig. 2 The Upper Plenum of the PGSFR

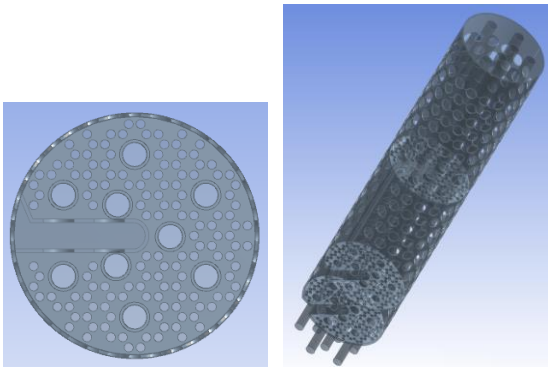

(a) First grid plate (b) UIS

Fig. 3 Shape of the first grid plate and the overall view of the UIS

Fig. 4 Numerical grid of fluid domain

3.3 Analysis results

The time-averaged velocity and temperature are obtained as computation results. Since the data of the temperature fluctuation with time are required for the

thermal striping, monitoring points for temperature fluctuation are set to some places shown in Fig. 5 and Fig 6. As shown in Fig. 5, the monitoring points on the plates of UIS are underneath the first plate and second plate. The side wall of each IHX has two monitoring points which are shown in Fig. 6.

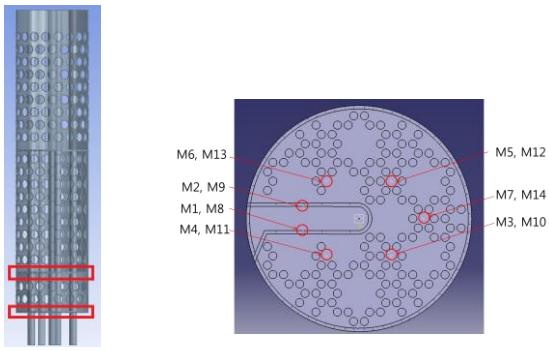

(a) Side of UIS (b) Monitoring points on the plates

Fig. 5 Monitoring points and its position

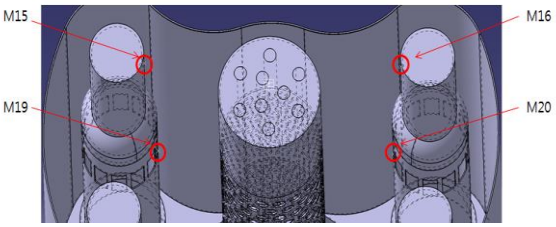

Fig. 6 Monitoring points on the side wall of IHX

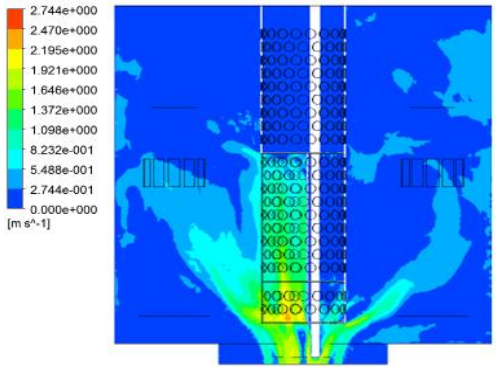

Fig. 7 Velocity contour (x-axis plane)

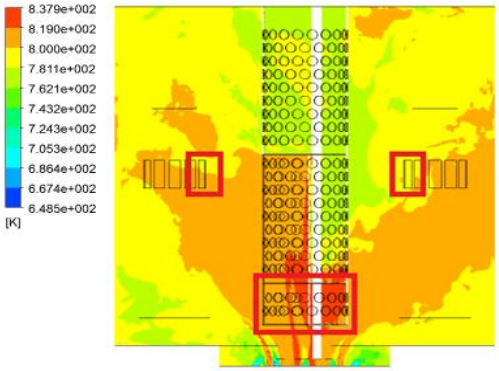

Fig. 8 Temperature contour (x-axis plane)

As the time-averaged variables, the contours of the time-averaged velocity and the temperature are presented in Fig. 7 and Fig. 8 respectively. Since the thermal hydraulic core design of the PGSFR is not settled down yet, the mass flow rate and temperature of the core outlet are provided from a tentative design. In these figures we can observe that the sodium flows from the reactor core flow into the inside of the UIS and flows out of the UIS mostly through the ⊃-shape region at the side of UIS. Some of the sodium flows through the opposite side of the UIS. Most of the temperature fluctuation in the UIS surfaces is observed at the three plates of the UIS and it is hardly seen above those plates. The flows from the reactor core are not mixed completely until they reach the UIS.

The time-averaged temperature distributions are plotted at four locations above the reactor core as shown in Fig. 9. The interval between the locations is around 150mm.

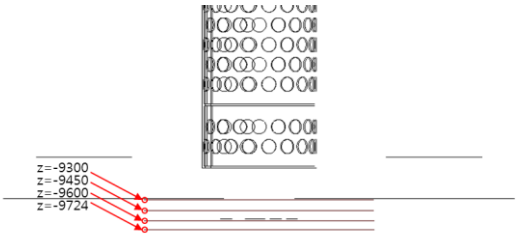

Fig. 9 The each elevation for temperature distribution

The predicted time-averaged temperature contours are given in Fig. 10 to Fig. 13. The temperature contour in Fig. 10 shows the temperature distribution of the core outlet just above the reactor core. The flows are mixed not only inside of the core outlet, but outside of the core region. Although the flow outside of the reactor core is gradually mixed as shown in Fig. 11, the temperature of sodium inside the reactor core region does not change much. The flow inside the reactor core region is highly mixed above a certain elevation as shown in Fig. 12 and Fig. 13. But the flow inside the reactor core region is not completely mixed, and reaches the first grid plate of the UIS. As a result, the thermal striping should be considered along the centroid of the reactor core region because the non-mixing flow can reach the structure of the UIS.

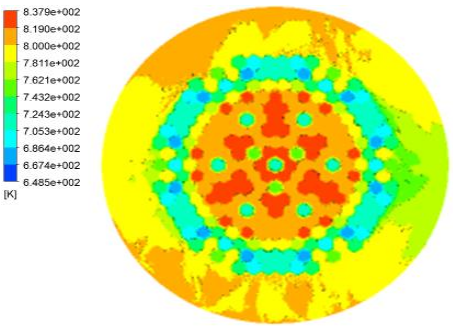

Fig. 10 Temperature contour at z=-9724mm

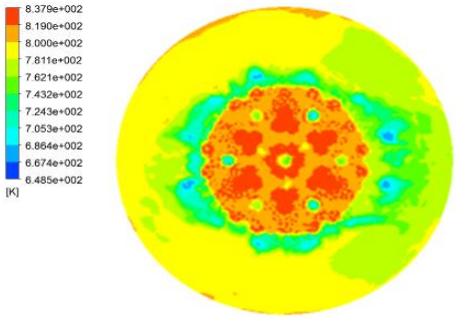

Fig. 11 Temperature contour at z=-9600mm

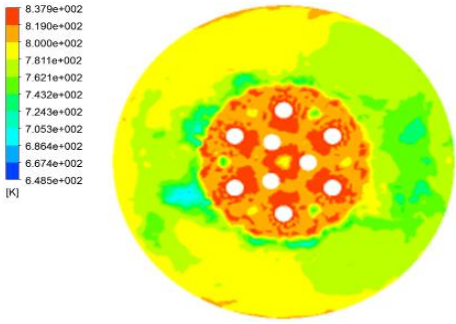

Fig. 12 Temperature contour at z=-9450mm

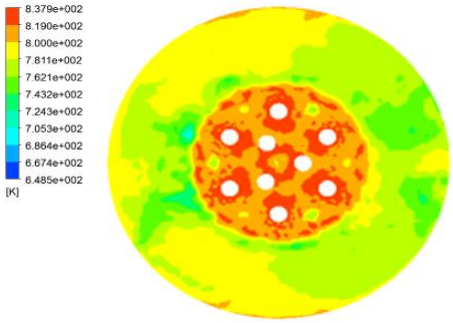

Fig. 13 Temperature contour at z=-9300mm

The time-averaged temperature distributions of the first and second plates of the UIS are given in Fig. 14 and Fig. 15. Fig. 14 shows that the non-mixing flow reaches the first plate as expected. In addition, as we have observed in Fig. 8, the flow is not completely mixed even when it reached the second plate of the UIS. Thus, the thermal striping at the second plate should be considered.

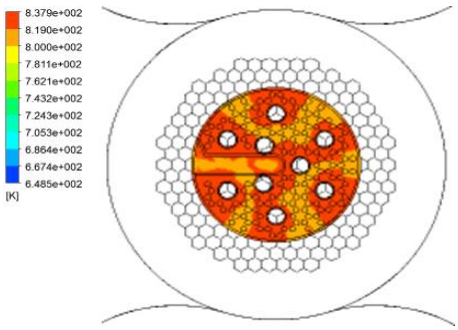

Fig. 14 Temperature contour at the first plate of UIS

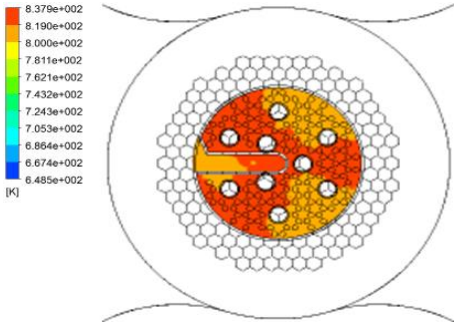

Fig. 15 Temperature contour at the second plate of UIS

The frequency and amplitude of the temperature fluctuation are the important parameters in the thermal striping analysis as mentioned before. In order to obtain these data, we set some monitoring points at the surfaces of the structures where there are possibilities for a large temperature fluctuation. The graphs below show the results of the simulation with the LES at a certain time interval (22s to 28). Some of these monitoring points are located at the side wall of each IHX and the time variations of temperature are plotted in Fig. 16. The frequency and amplitude of the temperature fluctuation show small differences among the locations. In this graph, the amplitude of temperature fluctuation at M16 and M19 locations is about 5 degrees and is less than that at the M15 and M20 locations. Since the frequency is not large at these locations, however, the thermal striping is not important at the IHX walls.

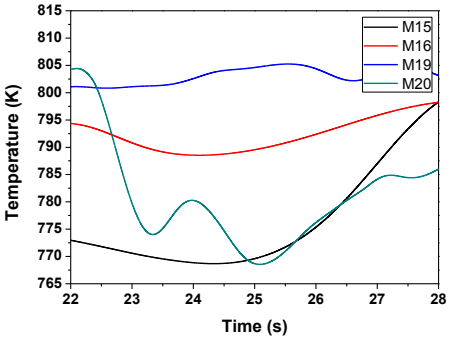

Fig. 16 Temporal variation of temperature at the surface of IHX

As we have already observed in the time-averaged velocity and the temperature distributions, some of the sodium in the UIS flows through the ⊃-shape region and flows out at the inlet of IHX. Therefore, the temperature fluctuation at this region needs to be observed. The temporal variation of temperature at the ⊃-shape region of the first and second plate are plotted in Fig. 17 (the locations are given in Fig. 5-(b)). In this plot, the black solid line is the M2 point and it is located at the second plate. The variation of temperature at the M2 point is less than that at the M9 point, which is located at the first plate. But the frequency and

amplitude of temperature fluctuation are not small at these points. Thus, these two points should be considered for a thermal striping analysis.

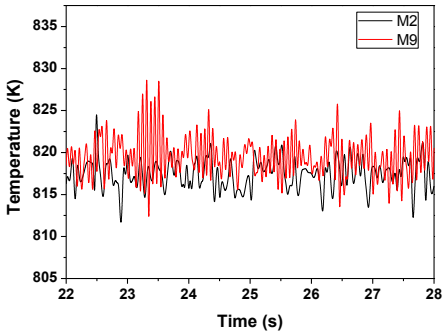

Fig. 17 Temporal variation of temperature for M2 and M9 points at the plate of UIS

As we have seen in the time-averaged temperature distribution, the difference between the first and second plates exists. The temporal variations of temperature at the first and second plates are plotted in Fig. 18 and Fig. 19 respectively. The frequency and amplitude of the temperature fluctuation are different among the locations, but the amplitude at the first plate reaches 10 degrees, whereas at the second plate it reaches 5 degrees. In the case of the M11 and M13 points, the amplitude is larger than that of the others. It seems that this is affected by the locations which are closed to the ⊃-shape region.

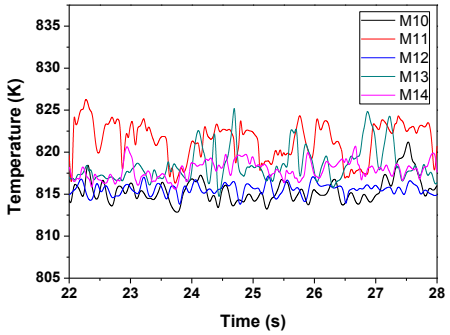

Fig. 18 Temporal variation of temperature for points in the first plate of UIS

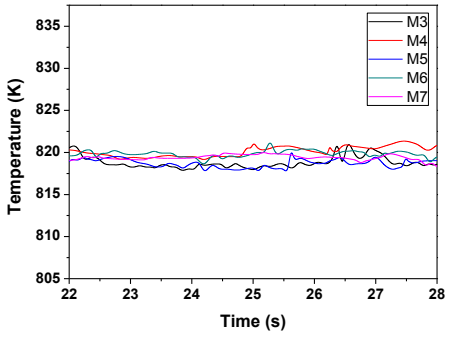

Fig. 19 Temporal variation of temperature for points in the second plate of UIS

3. Conclusions

The numerical investigation of the thermal striping is performed with the LES method using the CFX-13 commercial code, where the solution domain is the upper plenum of the PGSFR. As the first step, dozens of monitoring points are set to locations that are anticipated to cause thermal striping. Then, the temperature fluctuations were calculated along with the time-averaged variables such as the velocity and temperature. From these results we have obtained the following conclusions.

(1) At the side wall of IHX, a slight fluctuation is observed, but it seems that there is no risk of thermal striping.

(2) The flows from the reactor core are not mixed when reaching the UIS. So both the first and second plates need to be considered.

(3) Among the first grid plate regions, the ⊃-shape region is the weakest region for thermal striping. The second weakest region for thermal striping is the ⊃-shape region in the second grid plate of the UIS.

4. Acknowledgement

This work was supported by the National Research Foundation of Korea (NRF) grant funded by the Korea government (MSIP). (No. 2012M2A8A2025624)

REFERENCES

[1] Nam, H. Y. and Kim, J. M., 2004, "Thermal Striping Experimental Data," Internal Report, KAERI, LMR/IOC-ST-002-04-Rev.0/04.
[2] Chacko, S., Chung, Y. M., Choi, S. K., Nam, H. Y. and Jeong, H. Y., 2011, "Large-Eddy Simulation of Thermal Striping in Unsteady Non-isothermal Triple Jet," International Journal of Heat and Mass Transfer, 54, pp. 4400-4409.
[3] Shih, T. H., Liou, W. W., Shabbir, A., Yang, Z. and Zhu, J., 1995, "A New Eddy-Viscosity Model for High Reynolds Number Turbulent Flows - Model Development and Validation," Computer and Fluids, 24(3), pp. 227-238.
[4] Nicoud, F. and Ducros, F., 1999, "Subgrid-Scale Stress Modelling Based on the Square of the Velocity Gradient Tensor," Flow, Turbulence and Combustion, 62, pp. 183-200.